UBC ISCI 422 "Models in Science"

Project 3: Model Construction – Report

Developing an Innovative Nanopharmaceutical for Cancer Treatment

by

Jesse Popov

Abstract

I have developed a numerical computer model to help develop a drug technology (nanopharmaceutical) that is intended for use in cancer patients. The formulation that we have developed in our laboratory includes the drug trastuzumab, which is used to treat breast cancer, and we have found that our nanopharmaceutical is much more efficacious than trastuzumab alone. In an effort to explain these effects, we have turned to the lipid raft concept, a revolutionary new theory on the way that cellular membranes function. My model encompasses several aspects of the way that our nanopharmaceutical would be expected to interact with lipid rafts in the cell membrane, and has provided results that are readily and directly testable in our laboratory. I intend to experimentally verify these results to strengthen the assertions of the model.

1 Introduction

The goal of the work presented here is to further the development of a novel drug technology that can be used to treat cancer and increase the quality of life of cancer patients. As part of the breast cancer research program in our laboratory at the BC Cancer Research Centre, we study a drug called trastuzumab, which is used clinically in women with certain advanced-stage breast cancers [1]. In order to qualify for trastuzumab treatment, the cancer cells must overexpress the target of the drug, which is the protein ErbB2 (herein abbreviated as B2). B2 overexpression contributes directly to the oncogenic phenotype since it transmits growth signals to the cancer cell. By reversing this signalling, a regression of the cancerous state occurs [2].

It is interesting that the mechanism of action of trastuzumab is unclear [2]. It is known, however, that the drug binds strongly to B2 in the region close to the plasma membrane, disrupting associations with other ErbB family members including ErbB1 (B1) and ErbB3 (B3) [3]. Growth signals are created within the cell when the ErbB family members form dimers. This may happen spontaneously, or in response to growth factors such epidermal growth factor (EGF) or heregulin (Her). By disrupting dimerization with B1 and B3, trastuzumab attenuates B2 signalling, although it is unclear exactly how this happens [2].

In our laboratory, we have been developing a trastuzumab-containing pharmaceutical agent that works much better than trastuzumab itself. We have

termed it a nanopharmaceutical (NP), and Figure 1.1 contains a description of its composition.

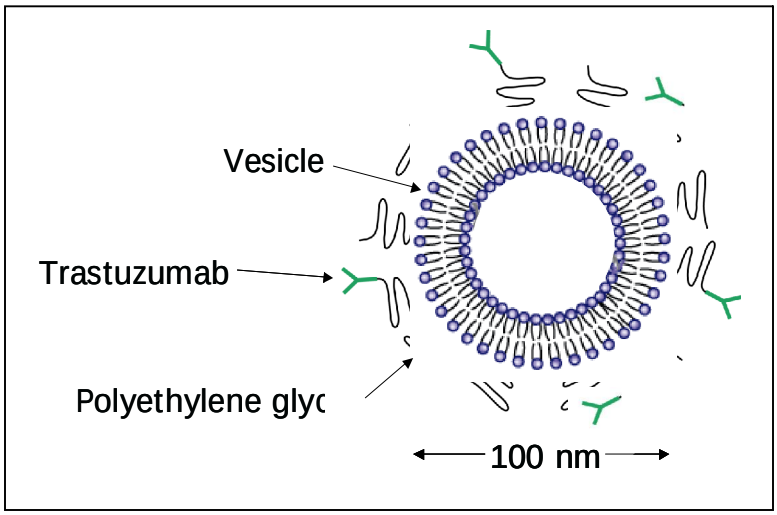

Figure 1.1 Two-dimensional representation of the nanopharmaceutical. The core of the nanopharmaceutical is small unilamellar vesicle that consists of a spherical phospholipid bilayer. Tethered to the vesicle are several polyethylene glycol chains, which serve to stabilize the vesicle and prolong its circulation lifetime. Finally, certain polyethylene glycol chains contain a molecule of trastuzumab bound to the end. The number of trastuzumab molecules (and hence ErbB2 binding sites) can be controlled and is generally in the region of 40 molecules (or 80 binding sites).

We have conducted *in vitro* and *in vivo* experiments that confirm that equimolar amounts of trastuzumab are an order of magnitude more efficacious when contained in the NP [manuscript in preparation]. Given the elusive nature of the mechanism of action of trastuzumab itself, however, we simply have a hypothesis at this point of how our NP exerts its effects. In creating this hypothesis, we have turned to the lipid raft concept.

Plasma membrane lipid rafts are small (< 100 nm), dynamic assemblies of specific lipids and proteins in the plane of the membrane bilayer [4]. Their composition depends in particular on three lipid species: sphingomyelin (SM),

cholesterol (Chol), and ganglioside GM1 (GM1) [5]. Rafts serve as small regions of confinement for many types of integral membrane proteins, particularly signalling proteins such as the ErbB family members [6]. As for raft association, B2 is of particular interest since some evidence suggests that this protein is inactive when associated with lipid rafts [7]. In this model, I assume that this is true, and this forms the overarching assumption upon which the entire model presented below is constructed.

We believe our NP serves to crosslink B2 on the cell surface, resulting in the formation of a NP-B2 complex. This complex enables stabilization of the raft phase such that the B2 bound to NP becomes sequestered in lipid rafts in the plasma membrane. Since B2 cannot transmit signals when in lipid rafts, the NP effectively inactivates B2 in this manner, reversing the oncogenic phenotype.

Clearly, a rigorous model for investigating this hypothesis would be beneficial, since the mechanism is multistep and involves many different combinations of lipid and protein molecules in the plasma membrane. I have constructed a computer model to investigate whether our NP can effectively sequester B2 in lipid rafts, and to see how this sequestration is affected by various external stimuli such as growth factor stimulation and raft disruption, two tools we currently use in experiments in our laboratory.

2 Methods

In order to investigate my hypothesis, I am using a model instead of physical experiments because it will allow the generation of a relatively large body of data without having to perform time-consuming and expensive experiments. In this way, I can target specific experimental conditions that I will determine from the results of my model.

I have chosen to use a numerical model since it lends itself well to the topic at hand. The processes involved in creating the model can be easily described using chemical equations and converted into differential equations using a framework of chemical reaction kinetics, as described in the next section.

2.1 Model Description

Each process implied in the hypothesis proposed for the nanopharmaceutical (NP) mechanism above was represented by one or more chemical equations. The 38 equations that were required in total can be found in Appendix B. They fall into four broad categories, for which the rate constants are colour-coded in Appendix B as follows: green, raft production and monomeric ErbB-raft association; blue, interactions of ErbB with growth factors; red, interactions involving NP; black, ErbB dimerization interactions. A schematic representation of these equations is found in Figure 2.1, and the theories and assumptions that went into creating them are discussed below.

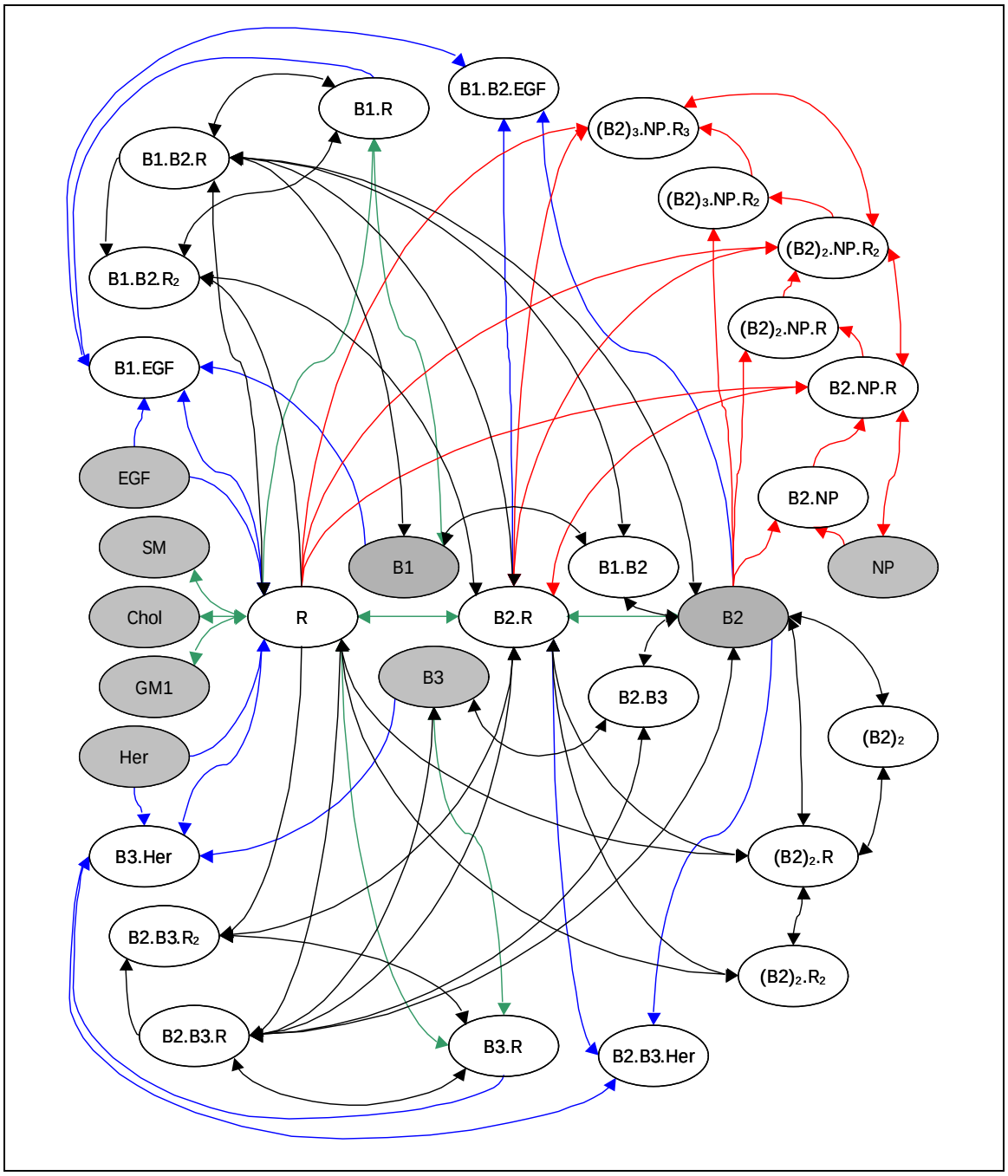

Figure 2.1 Flowchart depicting interconnectivity of the constituents of the model. An arrow between two species indicates that in Appendix B, there is a chemical reaction with the two components on either side of the arrow. Single-ended arrows represent one-way reactions, while double-ended arrows signify chemical equilibria. Species within shaded ovals are those for which initial values can be specified in the model; all other initial values are zero. Arrows are coloured as follows: green, raft production and monomeric ErbB raft association; blue, ErbB-growth factor interactions; red, ErbB2-raft-nanopharmaceutical interactions; black, ErbB dimerization reactions. See Appendix A for abbreviations.

In creating the model, chemical kinetics were assumed to apply. This means that the constituent molecules are present in sufficiently high concentrations and that they diffuse rapidly. I also assumed that the system was closed and that levels of transcription did not vary. This provided a closed-form solution for each set of conditions being tested. The concentrations of all components are relative and are expressed as the number of molecules per square unit of space in the plasma membrane. Rate constants are also relative and were assigned based on literature data, and can be found in the attached NetLogo file (see Appendix D).

The first step in creating the model was to simulate lipid raft production. Although rafts are composed of hundreds of types of lipid and protein molecules [4], the model only requires that three different lipid molecules come together, and in doing so, they create a lipid raft with three protein binding sites (with the binding sites represented as R in Figure 2.1 and Appendix B). Moreover, since rafts are short-lived and metastable [8], k_2 was assumed to be 10^6-fold higher than k_1 in equation (1).

Each of the ErbB family members (B1, B2, B3) were next assumed to interact with lipid rafts to roughly the same extent (eqs. (2) to (4)). Rate constants were set such that approximately half of each component was raft-associated in the absence of other interactions, consistent with the literature [7].

Equations (5) to (12) constitute the interactions of ErbB family members with growth factors. Epidermal growth factor (EGF) binds specifically to B1, and

heregulin (Her) binds to B3. These two interactions are strong [3] and were assumed to occur rapidly. Moreover, I assumed that the growth factors induce dissociation of B1 and B3 from lipid rafts (eqs. (6) and (10)), since growth-factor induced activation of ErbB coincides with ErbB-raft dissociation [7]. Once B1 and B3 were each bound to their growth factors, recruitment of B2 and formation of dimers were assumed to occur rapidly. Taken together, these interactions contribute to lowering the levels of raft-associated B2 upon stimulation by growth factors. It is important to note that B2 is inactive only when it is raft-associated.

Next, the action of the NP was modeled in equations (13) to (21), based on our hypothesis that the NP serves to sequester B2 in lipid rafts. The main assumption here is that each NP only has the ability to bind three B2 molecules, when in reality, the limit is upwards to 200. In these equations, there appears to be a complex array of chemical species, but this simply results from the assumed trivalent nature of the NP. Eqs. (13) and (15) show that in the absence of rafts, B2 and NP interact strongly and recruit a raft, while eq. (14) shows that the NP reversibly binds B2 if it is already raft-associated. Eqs. (16) to (18) and (19) to (21) mimic eqs. (13) to (15) in that they signify the recruitment of a second and third B2 molecule, respectively. Each subsequent B2 recruitment step was assumed to occur less rapidly than the preceding one.

Finally, the dimerization reactions of the ErbB family members were included in the model, since these play significant functional roles. Another

important level of organization is higher-order ErbB clusters of up to ~1000 molecules [7], but for simplicity, these were not included here. I have modeled B1-B2 dimerization in eqs. (22) to (27), as well as parallel sets of equations for B2-B3 dimerization (eqs. (28) to (33)) and B2 homodimerization (eqs. (34) to (38)). Although numerous, these equations represent the various combinations of dimers at different levels of raft association. Even though it does occur, I chose not to include B1-B3 dimers in the model since they present in significantly lower levels in the plasma membrane [7].

Once the chemical equations were devised, there became the task of deriving expressions for the rate of change of the concentration of each of the chemical components of the model. Briefly, an expression for this rate of change was determined for each component in all the equations, then the expressions for each distinct chemical species were summed. This is described in greater detail in Appendix C. Once the mathematical expressions for each of the 32 chemical species were found, they were inputted into the System Dynamics Modeler in NetLogo 3.1.4, completing the construction of the model and allowing verifications of the model to be performed.

2.2 Model Verification

With the model constructed, it was necessary to verify that it behaved as expected under certain conditions. For one, if any of the lipid components were absent, then no rafts should form, and there should be no raft-associated

components. Also, if any of B1, B2, or B3 are absent, there should be no downstream components that contain the missing protein. Both these conditions were found to be true.

Further verification tests included setting specific rate constants to zero and ensuring that no downstream chemical species were present, regardless of initial conditions. For example, k_{19} and k_{20} were set to zero, which are rate constants for the two initial reactions involving NP. As a result, no components that contained NP were formed. The same results were obtained when the initial NP value was set to zero. This type of test was repeated for several other components, which verified that the model behaved as expected.

This particular model fails, however, when any of the initial values are set higher than a given threshold. These values depend on the particular component. The error in the calculations occurred because there were numbers that were calculated that were too large for NetLogo to handle.

Due to the structure of this model, it is intuitively impossible for values for specific components to go above their initial values. This effect, however, is likely due to having set the time step too large (dt = 0.01). Given the iterative nature of the calculations, if the time step is too large (i.e. the time course is rather discontinuous), one calculation may result in a number being generated that is much larger than would be generated with a smaller time step. As successive calculations are performed, this large number is amplified until the results have no relevance. One solution would be to use a smaller time step, but

this makes the calculations prohibitively slow. Moreover, the upper thresholds for the initial values set a range of initial conditions from which useful results can be obtained using the larger time step.

2.3 Experiment Description

The goal of the following experiments on the model is to obtain relevant information that can be tested experimentally. As such, I set the initial B2 concentration an order of magnitude higher than those of B1 and B3, simulating B2 overexpression. Next, I incrementally increased the NP concentration in this B2-overexpressing scenario up to the threshold value, and in each case I determined the total amount of raft-associated B2. In NetLogo, I plotted the twelve chemical species that contained raft-associated B2 in the plot output. For each NP concentration, I allowed the system to reach equilibrium, then I exported the data to Excel and I determined the sum of the concentrations of these twelve components, which represented the total concentration of raft-associated B2. Finally, I plotted the raft-associated B2 concentration against the NP concentration in order to observe the effects of increasing NP concentration.

Next, I was interested in studying the extent to which growth factor stimulation or external raft disruption affected the ability of the NP to sequester B2 in rafts. Both raft disruption by depleting Chol and growth factor stimulation with EGF and/or Her are expected to cause B2 to dissociate from rafts. Keeping the NP concentration close to the threshold value that was determined in the first

experiment, I incrementally increased the growth factor concentrations (keeping EGF and Her concentrations the same) and I determined the raft-associated B2 concentration for each case, as before. In a separate experiment, I decreased the Chol concentration down to zero in the absence of growth factors. I present the data that I obtained below.

3 Results

The first set of results obtained from the experiments described in Section 2.3 is the effect of increasing NP concentration on the total levels of raft-associated B2. The NP concentration was increased to the threshold value of 0.5, and the results are presented in Figure 3.1.

This plot shows that the NP effectively causes B2 to remain within lipid rafts, and that the effect is more pronounced at higher NP concentrations. This is consistent with the notion that the NP serves to stabilize the raft phase by crosslinking B2. When only a few B2 molecules are crosslinked, the raft phase is less stable and more B2 molecules escape to the non-raft region of the membrane. More extensive crosslinking, however, results in greater stabilization of lipid raft regions, and B2 localization in these regions as a result of NP binding means that a much greater proportion of B2 will remain constitutively raft-associated.

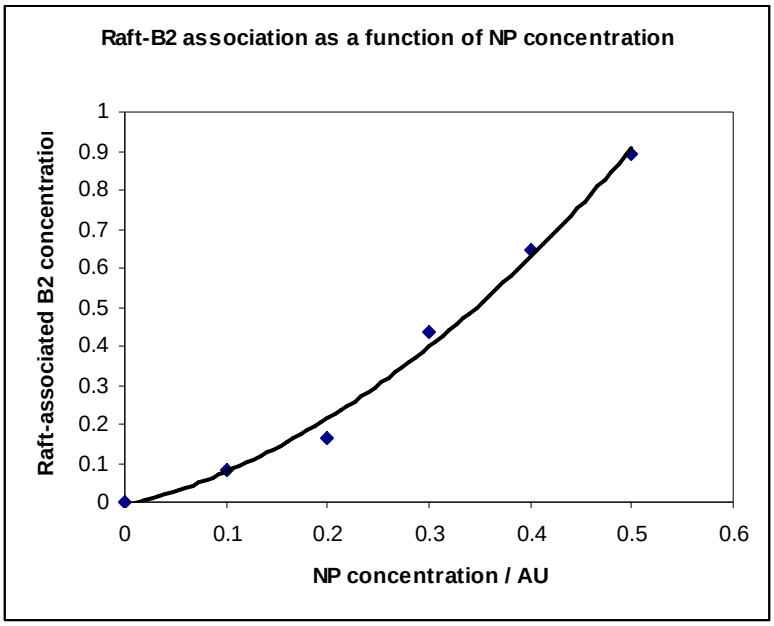

Figure 3.1 Levels of raft-associated B2 increase with NP concentration.

The next experiment involved investigating the ability of growth factors to interfere with the action of the NP. I increased the concentrations of EGF and Her incrementally and determined the total concentration of raft-associated B2, as described in Section 2.3. These results are shown in Figure 3.2.

As seen below, in B2-overexpressing cells, ErbB growth factors interfere with the ability of the NP to sequester B2 in rafts. This is reasonable since growth factor stimulation causes B2 to dimerize with other ErbB family members, making it inaccessible to NP binding. Also, growth-factor induced dimerization coincides with translocation from plasma membrane rafts [7]. The addition of growth factors, however, does not produce a striking result, only decreasing the level of raft-associated B2 to ~90% of its original value.

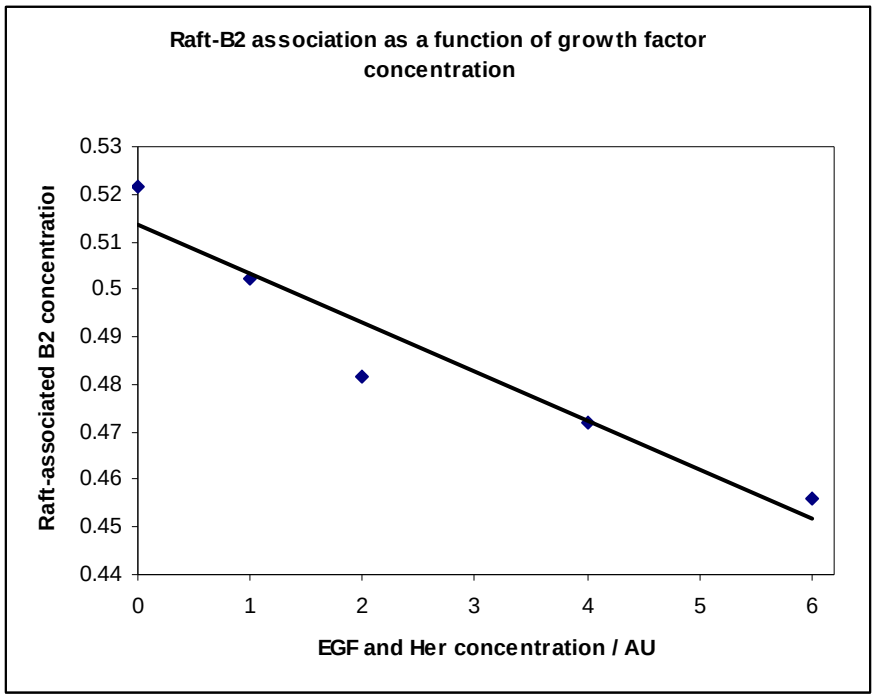

Figure 3.2 Levels of raft-associated B2 decrease with growth factor stimulation in the presence of NP.

On the other hand, the removal of a raft lipid more significantly affects the ability of the NP to contain the B2 within rafts. The data for this scenario is presented in Figure 3.3. Interestingly, this data does not fit well to any type of regression, which may be due to the fact that the chemical equation for raft production (Appendix B, eq. (1)) is a third-order reaction. It is clear, however, that the effects of Chol depletion are most pronounced only at low Chol levels. When a modest amount of Chol is removed, the effects are similar in magnitude to growth factor stimulation.

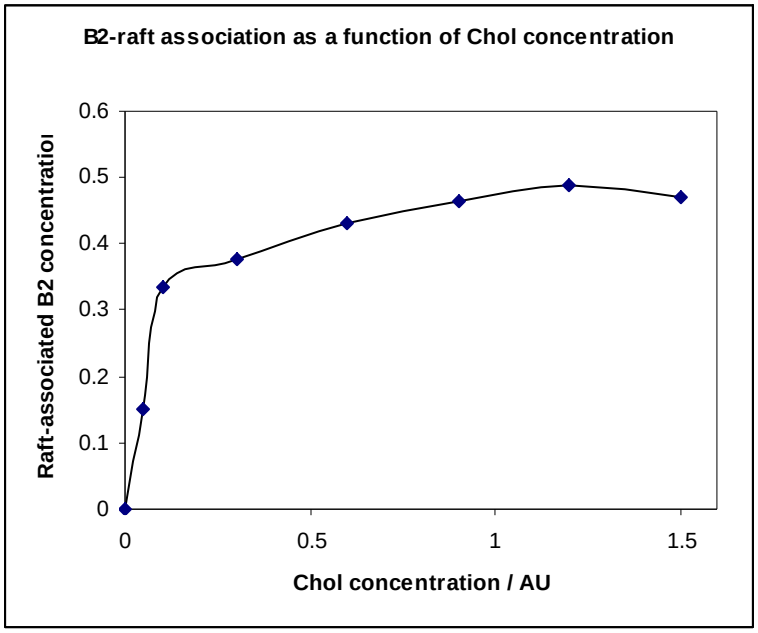

Figure 3.3 Levels of raft-associated B2 drop sharply at low Chol concentrations.

4 Discussion

The overall goal of the experiments described above was to obtain results that can be tested in our laboratory. Experimental validation would strengthen the implications of the model and lend credibility to its predictions. It would also indicate that the assumptions that went into the model were valid and that this model encompasses the dominant factors that influence the action of our NP.

All the results obtained above can be tested experimentally using one of several methods. I have opted to employ a technique developed by Gombos *et al.* [9], which uses flow cytometry to measure the level of raft association of a given protein. Using cell lines that overexpress B2, I am able to directly produce plots similar to Figures 3.1 to 3.3. Addition of growth factors is straightforward

and can be easily controlled, and cholesterol depletion can be performed with one of several agents, most commonly methyl-β-cyclodextrin.

One may wonder why it is even necessary to employ growth factors and/or cholesterol depletion. For one, including growth factors in experiments more closely approximates *in vivo* conditions. A tumour within an organism does not exist in a vacuum; it is in constant contact with the bloodstream, which feeds it with nutrients and external signals. Since growth factors strongly influence cancer progression, they must be included in pre-*in vivo* studies.

As for Chol depletion, it is a very common tool used in the study of lipid rafts. Its purpose is twofold; first, it serves to liberate raft-associated proteins, enabling a measure of the strength of raft association by comparing the normal and cholesterol-depleted states. Second, it serves as a control, since no proteins should be raft associated under conditions of extreme cholesterol depletion.

4.1 Summary

We were very happy to observe initially that our trastuzumab-containing nanopharmaceutical worked much better than trastuzumab alone. At the same time, our job has been made difficult since the mechanism of action of trastuzumab is not definitively known. We believe with good reason, however, that our nanopharmaceutical exerts its effects by sequestering B2 in lipid rafts, effectively turning off its cancer-inducing properties. The model that I have developed here encompasses several aspects of this hypothesis and the results

that it provides lend themselves well to being tested in the laboratory. Experimental validation of these results would lend a great deal of credibility to our hypothesis. This would then jumpstart an effort to further tailor our formulation in response to a more concrete mechanism of action, further enhancing its already pronounced effects.

Page limit (12-16 pages, excluding references and appendices) enforced to this point. Do not delete.

References

1. Cobleigh, M.A., et al., *Multinational study of the efficacy and safety of humanized anti-HER2 monoclonal antibody in women who have HER2-overexpressing metastatic breast cancer that has progressed after chemotherapy for metastatic disease.* J Clin Oncol, 1999. **17**(9): p. 2639-48.
2. Nahta, R. and F.J. Esteva, *Herceptin: mechanisms of action and resistance.* Cancer Lett, 2006. **232**(2): p. 123-38.
3. Vereb, G., et al., *Signaling revealed by mapping molecular interactions: implications for ErbB-targeted cancer immunotherapies.* Clin Applied Imunol Rev, 2002. **2**: p. 169-86.
4. Simons, K. and E. Ikonen, *Functional rafts in cell membranes.* Nature, 1997. **387**(6633): p. 569-72.
5. Simons, K. and W.L. Vaz, *Model systems, lipid rafts, and cell membranes.* Annu Rev Biophys Biomol Struct, 2004. **33**: p. 269-95.
6. Simons, K. and D. Toomre, *Lipid rafts and signal transduction.* Nat Rev Mol Cell Biol, 2000. **1**(1): p. 31-9.
7. Nagy, P., et al., *Lipid rafts and the local density of ErbB proteins influence the biological role of homo- and heteroassociations of ErbB2.* J Cell Sci, 2002. **115**: p. 4251-62.
8. Rajendran, L. and K. Simons, *Lipid rafts and membrane dynamics.* J Cell Sci, 2005. **118**(Pt 6): p. 1099-102.
9. Gombos, I., et al., *Cholesterol sensitivity of detergent resistance: a rapid flow cytometric test for detecting constitutive or induced raft association of membrane proteins.* Cytometry A, 2004. **61**(2): p. 117-26.

Appendix A: Abbreviations

B1	ErbB1
B2	ErbB2
B3	ErbB3
Chol	Cholesterol
EGF	Epidermal growth factor
GM1	Ganglioside GM1
Her	Heregulin
NP	Nanopharmaceutical
R	Raft binding site for protein
SM	Sphingomyelin

Combinations of the above serve to define distinct chemical species. For example:

B1.R = Raft-associated ErbB1

B1.B2.EGF = Epidermal growth factor bound to both ErbB1 and ErbB2

$(B2)_2$.NP.R_2 = Complex of nanopharmaceutical and two raft-associated ErbB2 molecules

Appendix B: Chemical Equations

The following reactions serve as the basis for the model presented in this paper. Rate constants are coloured to correspond to the arrows in Figure 2.1.

$$\mathbf{SM} + \mathbf{Chol} + \mathbf{GM1} \underset{k_2}{\overset{k_1}{\rightleftharpoons}} 3\,\mathbf{R} \quad (1)$$

$$\mathbf{B1} + \mathbf{R} \underset{k_4}{\overset{k_3}{\rightleftharpoons}} \mathbf{B1.R} \quad (2)$$

$$\mathbf{B2} + \mathbf{R} \underset{k_6}{\overset{k_5}{\rightleftharpoons}} \mathbf{B2.R} \quad (3)$$

$$\mathbf{B3} + \mathbf{R} \underset{k_8}{\overset{k_7}{\rightleftharpoons}} \mathbf{B3.R} \quad (4)$$

$$\mathbf{B1} + \mathbf{EGF} \xrightarrow{k_9} \mathbf{B1.EGF} \quad (5)$$

$$\mathbf{B1.R} + \mathbf{EGF} \xrightarrow{k_{10}} \mathbf{B1.EGF} + \mathbf{R} \quad (6)$$

$$\mathbf{B1.EGF} + \mathbf{B2} \xrightarrow{k_{11}} \mathbf{B1.B2.EGF} \quad (7)$$

$$\mathbf{B1.EGF} + \mathbf{B2.R} \underset{k_{13}}{\overset{k_{12}}{\rightleftharpoons}} \mathbf{B1.B2.EGF} + \mathbf{R} \quad (8)$$

$$\mathbf{B3} + \mathbf{Her} \xrightarrow{k_{14}} \mathbf{B3.Her} \quad (9)$$

$$\mathbf{B3.R} + \mathbf{Her} \xrightarrow{k_{15}} \mathbf{B3.Her} + \mathbf{R} \quad (10)$$

$$\mathbf{B3.Her} + \mathbf{B2} \xrightarrow{k_{16}} \mathbf{B2.B3.Her} \quad (11)$$

$$\mathbf{B3.Her} + \mathbf{B2.R} \underset{k_{18}}{\overset{k_{17}}{\rightleftharpoons}} \mathbf{B2.B3.Her} + \mathbf{R} \quad (12)$$

$$\mathbf{B2} + \mathbf{NP} \xrightarrow{k_{19}} \mathbf{B2.NP} \quad (13)$$

$$\mathbf{B2.R} + \mathbf{NP} \underset{k_{21}}{\overset{k_{20}}{\rightleftharpoons}} \mathbf{B2.NP.R} \quad (14)$$

$$\mathbf{B2.NP} + \mathbf{R} \xrightarrow{k_{22}} \mathbf{B2.NP.R} \quad (15)$$

$$\mathbf{B2.NP.R} + \mathbf{B2} \xrightarrow{k_{23}} \mathbf{(B2)_2.NP.R} \quad (16)$$

$$\mathbf{B2.NP.R} + \mathbf{B2.R} \underset{k_{25}}{\overset{k_{24}}{\rightleftharpoons}} \mathbf{(B2)_2.NP.R_2} \quad (17)$$

$$\mathbf{(B2)_2.NP.R} + \mathbf{R} \xrightarrow{k_{26}} \mathbf{(B2)_2.NP.R_2} \quad (18)$$

$$\mathbf{(B2)_2.NP.R_2} + \mathbf{B2} \xrightarrow{k_{27}} \mathbf{(B2)_3.NP.R_2} \quad (19)$$

$$\mathbf{(B2)_2.NP.R_2} + \mathbf{B2.R} \underset{k_{29}}{\overset{k_{28}}{\rightleftharpoons}} \mathbf{(B2)_3.NP.R_3} \quad (20)$$

$$(B2)_3.NP.R_2 + R \xrightarrow{k_{30}} (B2)_3.NP.R_3 \quad (21)$$

$$B1 + B2 \underset{k_{32}}{\overset{k_{31}}{\rightleftharpoons}} B1.B2 \quad (22)$$

$$B1.B2 + R \underset{k_{34}}{\overset{k_{33}}{\rightleftharpoons}} B1.B2.R \quad (23)$$

$$B1.R + B2 \underset{k_{36}}{\overset{k_{35}}{\rightleftharpoons}} B1.B2.R \quad (24)$$

$$B1 + B2.R \underset{k_{38}}{\overset{k_{37}}{\rightleftharpoons}} B1.B2.R \quad (25)$$

$$B1.B2.R + R \xrightarrow{k_{39}} B1.B2.R_2 \quad (26)$$

$$B1.R + B2.R \underset{k_{41}}{\overset{k_{40}}{\rightleftharpoons}} B1.B2.R_2 \quad (27)$$

$$B2 + B3 \underset{k_{43}}{\overset{k_{42}}{\rightleftharpoons}} B2.B3 \quad (28)$$

$$B2.B3 + R \underset{k_{45}}{\overset{k_{44}}{\rightleftharpoons}} B2.B3.R \quad (29)$$

$$\mathbf{B2.R} + \mathbf{B3} \underset{k_{47}}{\overset{k_{46}}{\rightleftharpoons}} \mathbf{B2.B3.R} \quad (30)$$

$$\mathbf{B2} + \mathbf{B3.R} \underset{k_{49}}{\overset{k_{48}}{\rightleftharpoons}} \mathbf{B2.B3.R} \quad (31)$$

$$\mathbf{B2.B3.R} + \mathbf{R} \xrightarrow{k_{50}} \mathbf{B2.B3.R_2} \quad (32)$$

$$\mathbf{B2.R} + \mathbf{B3.R} \underset{k_{52}}{\overset{k_{51}}{\rightleftharpoons}} \mathbf{B2.B3.R_2} \quad (33)$$

$$2\,\mathbf{B2} \underset{k_{54}}{\overset{k_{53}}{\rightleftharpoons}} \mathbf{(B2)_2} \quad (34)$$

$$\mathbf{(B2)_2} + \mathbf{R} \underset{k_{56}}{\overset{k_{55}}{\rightleftharpoons}} \mathbf{(B2)_2.R} \quad (35)$$

$$\mathbf{B2.R} + \mathbf{B2} \underset{k_{58}}{\overset{k_{57}}{\rightleftharpoons}} \mathbf{(B2)_2.R} \quad (36)$$

$$\mathbf{(B2)_2.R} + \mathbf{R} \xrightarrow{k_{59}} \mathbf{(B2)_2.R_2} \quad (37)$$

$$2\,\mathbf{B2.R} \underset{k_{61}}{\overset{k_{60}}{\rightleftharpoons}} \mathbf{(B2)_2.R_2} \quad (38)$$

Appendix C: Sample Differential Equation Derivation

The derivation of the equation for the rate of change of ErbB3 with respect to time is presented here. Similar calculations were performed for each chemical constituent in the model.

ErbB3 is found in equations (4), (9), (28), and (30). From each equation, the expression for $d[\mathbf{B3}]/dt$ will the product of the rate constant and the concentrations of components that contribute to its creation or disappearance. Increases and decreases in concentrations are denoted with positive and negative signs, respectively.

With square brackets denoting concentrations of constituents, the expression for $d[\mathbf{B3}]/dt$ from each equation is as follows:

From (4): $k_8[\mathbf{B3.R}] - k_7[\mathbf{B3}][\mathbf{R}]$

From (9): $-k_{14}[\mathbf{B3}][\mathbf{Her}]$

From (28): $k_{43}[\mathbf{B2.B3}] - k_{42}[\mathbf{B2}][\mathbf{B3}]$

From (30): $k_{47}[\mathbf{B2.B3.R}] - k_{46}[\mathbf{B2.R}][\mathbf{B3}]$

Overall, then:

$$\frac{d[\mathbf{B3}]}{dt} = k_8[\mathbf{B3.R}] - k_7[\mathbf{B3}][\mathbf{R}] - k_{14}[\mathbf{B3}][\mathbf{Her}] + k_{43}[\mathbf{B2.B3}] - k_{42}[\mathbf{B2}][\mathbf{B3}] + k_{47}[\mathbf{B2.B3.R}] - k_{46}[\mathbf{B2.R}][\mathbf{B3}]$$

Appendix D: NetLogo Code

Please see the attached file, “POPOV isci 422 project 3.nlogo”.

Grading Rubric

Both instructors will grade your work independently according to the criteria below (may not have equal weight). The final grade will be assigned by normalizing each instructor's evaluations (over all submissions) to have the same mean and variance (decided based on overall class performance), and averaging both instructors' normalized grades.

	Raw Score		
	Instructor:	Instructor:	
Criterion			**Comments**
Student worked independently without requiring too much instructor assistance.			
Motivation and research question clear and interesting from a scientific perspective.			
Model clearly explained.			
Model original and ambitious.			
Assumptions are thoroughly considered and well justified.			
Experiments are appropriate to answer research question.			
Experimental results clearly explained.			
Thoroughly explores implications of results and insights gained in regard to research question.			
The page limits were satisfied.			
Total =			Final Grade: